Conference Paper, Published Version

Ong, Muk Chen; Lim, Siow-Yong; Yu, Guoliang; Tan, Soon-Keat
Abutment Scour Using Lightweight Bed Material

Abutment Scour Using Lightweight Bed Material

Muk Chen Ong[1], Siow Yong Lim[2], Guoliang Yu[3], and Soon Keat Tan[4]

[1]*Research Engineer, Maritime Research Centre, School of Civil & Environmental Engrg., Nanyang Technological University, Singapore 639798. E-mail: cmcong@ntu.edu.sg.*
[2]*Assoc. Prof., School of Civil & Environmental Engrg., Nanyang Technological University, Singapore 639798. E-mail: csylim@ntu.edu.sg.*
[3]*Research Fellow, Maritime Research Centre, School of Civil & Environmental Engrg., Nanyang Technological University, Singapore 639798. E-mail: cglyu@ntu.edu.sg.*
[4]*Assoc. Prof. and Director of Maritime Research Centre, School of Civil & Environmental Engrg., Nanyang Technological University, Singapore 639798. E-mail: ctansk@ntu.edu.sg.*

ABSTRACT

This paper presents the results of abutment scour using lightweight bed materials (specific gravity 1.05). The near-bed flow structures around the abutment edge with scour hole were investigated. Generally, the flow around the toe of abutment edge consists of an upward helical flow which is the result of the combined vortices caused by the stream flow passing the abutment edge and the vertically rotating vortices due to the downflows. Along the edge of the abutment, the vortices become stronger with depth. Logically, the strength of vortices is zero at or near the bed. Thus, the strength of the vortices will attain a maxima at a certain small distance above the bed. The characteristics of sediment deposition downstream of the abutment are also discussed in this paper.

Based on dimensional analysis, a new model of the equilibrium clear water scour depth at the abutment is presented. The model indicates that the sediment density and densimetric Froude number are the two most important governing parameters in abutment scour. Experimental data of maximum clear water scour depth collected from the present study and other sources were analyzed and compared with the proposed model. Good agreement between the computed and measured maximum equilibrium scour depths was obtained.

Keywords: Lightweight materials, abutment scour, flow structure, densimetric Froude number.

INTRODUCTION

A common cause of bridge failures is due to pier and abutment scour during floods. Although significant advances have been made over the past decades, pier and abutment scour remains a problem of great engineering concern. Many studies on abutment scour have been conducted (Liu et al 1961; Laursen 1963; Gill 1972; Kwan 1984, 1988; Rajaratnam et al 1983; Tey 1984; Kandasamy 1989; Melville 1992, 2000; Dongol 1994 and Lim 1997). These studies were performed using natural sand. While many

researchers have performed detailed studies on the 3D flow structure for pier scour; there are only a handful of reported studies for abutment scour. Liu et al.(1961), Wong (1982) and Kwan(1988) performed the studies on the flow structures at short abutments. Kwan (1988) found that the vortex system remains the same irrespective of the flow depth. A summary on the flow structure of abutment scour was conducted by Melville and Coleman (2000). In the present study, the phenomena were investigated in greater details. Special attention was paid to the flow structure near the immediate edge of the abutment.

Garde et al (1961), Liu et al. (1961), Laursen (1963), Gill (1972), Froelich (1989), Melville (1992) and Lim (1997) proposed formulae to predict the equilibrium clear water scour. Quartz sediment was used in these laboratory-scale experiments.

This paper deals with the use of lightweight material as the model sediment. The first issue is to address the flow patterns and the flow structure at the abutment. Secondly, in order to correctly predict the equilibrium maximum clear water scour for non-quartz model sediment, a new model is developed. This new model takes into the effect of sediment density in the scour formation.

EXPERIMENTAL SETUP AND INVESTIGATIONS

A large open channel flume (30m long, 6m wide and 0.6m high) was used to investigate the flow structure and scouring process around an abutment. Two pumps were used to generate flow of up to 200 l/s. Sharp-crested weir was installed at the entrance of the flume to measure the flow rate. Three manometers were attached to the sidewall of the flume to measure the water surface level. A group of 8 sluice gates was installed as tailgates to control the water level in the flume. The experimental setup is shown in Figure 1.

The first 4 m of the channel bed from the entrance was paved with 10 mm - 20 mm gravels in order to generate fully developed flows. The remaining channel bed was paved with lightweight plastic material (specific gravity 1.05). The material is uniform in size and is cylindrical in shape (3.1 mm in diameter and 2.8 mm long). The thickness of the paved bed was 20 cm.

Altogether, 19 tests were conducted. The flow rate ranged from 88 l/s to 153 l/s. The abutment (placed at the left bank, as viewed in the direction of the stream flow) length varies from 7 cm to 88 cm. The abutments were installed perpendicularly to the sidewall of the flume. The experiment started by submerging all the plastic materials first and then the flow rate and depth were adjusted to the pre-determined values. The scour depth at the abutment was monitored continuously for 2 days. During the experiment, blue dye was used to aid in flow visualisation. The hydraulic parameters of the experiments are summarised in Table 1.

FLOW STRUCTURES AROUND ABUTMENT SCOUR

Figure 2 shows the streamflow patterns around the abutment. The flow deceleration ahead of the abutment creates a downward pressure gradient at the frontal face of the abutment and hence the downflows. The downflows dive towards the bed and generates vertical vortices. Simultaneously, the stream-wise flow is diverted towards the centreline of the flume. The diverted flow interacts with the approaching main stream flow and a series of planar vortices are formed. These vortices follow the right hand rule with the thumb pointing upwards (See Figures 3a-3c). The vortices formed intermittently at the abutment head, and they subsequently detached from the abutment edge and travelled further downstream.

The strength of the vortices at the edge of the abutment was investigated qualitatively using blue dye as visualisation aids. Figures 3a to 3c show that the vortice becomes stronger with depth. The entrainment power is also larger nearer the bed. Logically, the strength of the vortices should reduce to zero at the bed. Therefore, one would expect a maxima at a certain distance above the bed

At the location near the bed and around the toe of the abutment, the diverted stream-wise flow which approaches the edge of the abutment interacts with the vertical vortices (caused by the downflows) and the horizontal rotating vortices near the bed. These vortices and flow combined to form an intermittent, upward helical flow with a direction following the right hand rule with the thumb pointing upwards. The helical flow behaves like a mini tornado entraining particles from the bed. The radius of the helical flow is larger near the bed and gradually decreases in the vertical direction. This helical flow travels downstream of the abutment and towards the bank (same side with the abutment). The strength of the helical flow decreases while translating and rotating. A schematic sketch of the upward helical flow has been shown in Figure 2.

The downflows at the right (free stream end) frontal zone of the abutment dislodge sediments from the bed and the entrained sediments are carried by the vertical vortices helically towards the toe of the abutment. At the edge of the abutment, the sediments are swept upwards by the helical flow and transported downstream in the same helical path. They are deposited downstream when the strength of the upward helical flow weakens.

During the development of the scour hole at the abutment, bed materials are continuously being eroded from the entrainment zone adjacent to the abutment. The scour hole enlarges with time and erosion ceases when the slope of the scour hole is close to the repose angle (submerged) of the bed material. The strong vortices in the entrainment zone generate secondary vortices with the opposite rotating direction around the bow of the entrainment zone. The strength of these secondary vortices is not as strong. The results is the formation of a mild ridge surrounding the principal scour hole, as shown in Figure 4. The flow patterns are similar to Kwan's (1984) observation. Sediment deposition is also observed downstream and behind the abutment head. As the scour hole develops, the zone of deposition moves downstream until the scouring process reaches equilibrium. As the ridge of the sediment deposition grows, flow separation occurs at the crest of the

deposition. The separated flow dives into the mobile bed and starts to scour the bed. A dune is formed downstream of this ridge, and the crest is small. Figure 5 shows the formation of the two scour holes. The second scour hole tends to curl towards the (left) bank as a result of the helical flow.

The scouring mechanism is similar for both long and short abutments. For the long abutment, it was observed that there is a reversed eddy at the lee zone of the abutment near to the bank. The re-circulating eddy is weak and has negligible effect on the bank.

PREDICTION OF ABUTMENT SCOUR

Dimensional Considerations

Assuming the channel contraction effects are negligible, a dimensional analysis of the governing variables affecting the maximum local scour depth at an abutment yields

$$\frac{d_{se}}{y} = f(\frac{L}{y}, F_d, \frac{D_{50}}{y}, \frac{\gamma_s - \gamma}{\gamma_s}, \sigma_g, K_s, K_\theta, K_g) \qquad (1)$$

where d_{se}= maximum equilibrium scour depth ; y = water depth ; L= projected length of abutment; F_d = sediment densimetric Froude number, $u_1/\sqrt{[(S-1)gD_{50}]}$; u_1 = mean approach velocity; S = specific gravity of sediment = $\rho s/\rho$; D_{50} = median grain diameter; γ_s = specific weight of sediment; γ = specific weight of water; $(\gamma_s-\gamma)/\gamma_s$ = ratio of buoyant sediment weight to the actual sediment weight; σ_g = geometric standard deviation of the sediment-size distribution; K_s = shape factor; K_θ = alignment of the abutment ; K_g = factor representing the effects of approach channel geometry, such as floodplain.

In order to consider the importance of the density effect on the abutment scour, F_d, is used as one of the governing parameters instead of the fluid Froude number, $F_r = u_1/\sqrt{(gy)}$. The term, $(\gamma_s-\gamma)/\gamma_s$, is also included in Eqn. (1) to highlight the significance of the sediment weight.

Table 1 shows a summary of 30 experiments conducted in NTU, of which 19 sets were conducted using lightweight bed material, and 11 sets were quoted from Lim (1997). Sand was used in the latter study. All the tests in Table 1 were conducted with vertical-wall abutments under clear-water scouring conditions in rectangular channel. Hence, K_g = 1. The alignment angle of the abutment was 90°, i.e. K_Θ =1. The effect of σ_g was not considered as uniform non-cohesive sediments were used. Therefore the last 4 terms on the right side of Eqn. (1) can be dropped in the following analysis.

Data Analysis and Results

Based on Eqn. (1) and using multiple non-linear regression analysis, the following equation with a correlation coefficient R = 0.932 is obtained:

$$\frac{d_{se}}{y} = 1.86 \left(\frac{L}{y}\right)^{0.92} (F_d)^{1.41} \left(\frac{D_{50}}{y}\right)^{0.32} \left(\frac{\gamma_s - \gamma}{\gamma_s}\right)^{0.4} \tag{2}$$

To account for the different abutment shapes and alignment to the flow direction, we used $K_s{}^*$ and $K_\theta{}^*$ proposed by Melville (1992) where $K_s{}^*$ is the modified shape factor and $K_\theta{}^*$ is the modified alignment factor. Eqn. (2) becomes
.

$$\frac{d_{se}}{y} = 1.86 K_s{}^* K_\theta{}^* \left(\frac{L}{y}\right)^{0.92} (F_d)^{1.41} \left(\frac{D_{50}}{y}\right)^{0.32} \left(\frac{\gamma_s - \gamma}{\gamma_s}\right)^{0.4} \tag{3}$$

Figure 6 shows a comparison between the predicted d_{se}/y using Eqn. (2) and the measured d_{se}/y based on the data listed in Table 1. Most of the data fall within the band of ± 30 % from the line of perfect agreement.

Figure 7 shows a comparison between the predicted scour depth and the measured scour depths reported by other researchers. Some of experiments were not conducted using vertical wall abutments, and Eqn.(3) is used for these sets of data. Generally, except for the data set by Tey's (1984), the agreement is reasonable,.

Comparison of Abutment Scour Equations

To see whether existing equations can be used for data with lightweight bed materials, the writers selected Melville's (1992) and Lim's (1997) equations to validate the significant effect of F_d and $(\gamma_s-\gamma)/\gamma_s$ on abutment scour if lightweight materials had been used as bed sediments.

(a) Melville's Equation (1992)

$$d_{se} = 2K_s L \ , \qquad\qquad \frac{L}{y} < 1 \tag{4a}$$

$$\frac{d_{se}}{y} = 2K_s{}^* K_\theta{}^* \left(\frac{L}{y}\right)^{0.5} , \qquad\qquad 1 \le \frac{L}{y} \le 25 \tag{4b}$$

$$d_{se} = 10K_\theta y \ , \qquad\qquad \frac{L}{y} > 25 \tag{4c}$$

Figure 8 shows that Melville's equation over-predicts the abutment scour with lightweight sediments by more than 100%. His equation was formulated using quartz sediment as bed materials and the terms, F_d and $(\gamma_s-\gamma)/\gamma_s$, were not included in the equations.

(b) Lim's Equation (1997)

$$\frac{d_{se}}{y} = K_s (0.9X - 2) \ , \quad X > 2.22$$

$$where \ \ X = \left\{ (\theta_c)^{-0.375} (F_d)^{0.75} \left(\frac{d_{50}}{y} \right)^{0.25} \left[0.9 \left(\frac{L}{y} \right)^{0.5} + 1 \right] \right\}$$

(5)

Comparison between the Lim's predicted scour depth and actual measured scour depth is also shown in Figure 8. It is seen that Lim's equation also over-predicts the scour depth measured in the present study, albeit less conservative than Melville's. This is plausibly due to the inclusion of F_d in Lim's equation.

The term F_d alone is not enough to account for the effect of sediment density. The writers have introduced an additional parameter, $(\gamma_s - \gamma)/\gamma_s$ which has been shown to predict well the scour depth using both lightweight material and sand as model sediments.

CONCLUSIONS

The flow structure around an abutment has been investigated. The flow around the toe of the abutment edge consists of an upward helical flow which is the result of the combined vortices caused by the stream flow passing the edge of the abutment and the vertically rotating vortices due to the downflows. Along the edge of the abutment, the vortices become stronger with depth, reaches a maximum a certain small distance above the bed. The characteristic of the sediment deposition at downstream of the abutment is also discussed.

This study also shows that for investigation of abutment scour using lightweight material, the governing parameters are the densimetric Froude number F_d and the relative density term, $(\gamma_s - \gamma)/\gamma_s$. The present study emphasizes the density effect of bed sediments on abutment scour investigation.

To this end, a new model for predicting the maximum equilibrium clear-water abutment scour has been proposed. The study shows that the existing equations such as Melville's (1992) and Lim's (1997) are not applicable for determining the scour depth when the bed sediment are lightweight materials, simply because the density effect has not been accounted for adequately.

REFERENCES

Dongol, D. M. S.(1994). " Local scour at bridge abutments." *Rep. No. 544*, School of Engrg., Univ. of Auckand, New Zealand.

Froehlich, D.C.(1989). " Local scour at bridge abutments." *Proc.,ASCE Nat. Hydr. Conf.*, ASCE, New York, N.Y., 13-18

Garde, R. J., Subramanya, K., and Nambudripad, K. D. (1961). " Study of scour around spur dikes." *J. Hydr. Div.,* ASCE, 87(6), 23-38.

Gill, M. A. (1972). " Erosion of sand beds around spur dikes." *J. Hydr Div.,* ASCE, 98(9), 1587-1602.

Kandasamy, J. K. (1989). "Abutment scour." *Rep. No. 458*, School of Engrg., Univ. of Auckland, Auckland, New Zealand.

Kwan, T. F. (1984). "Study of abutment scour." *Rep. No. 328*, School of Engrg., Univ. of Auckland, Auckland, New Zealand.

Kwan, T. F. (1988). "A study of abutment scour." *Rep. No. 451*, School of Engrg., Univ. of Auckland, Auckland, New Zealand.

Laursen, E. M. (1963). " Analysis of relief bridge scour." *J. Hydr. Div.*, ASCE, 89(3), 93-118.

Lim, S. Y. (1997). "Equilibrium clear-water scour around an abutment." *J. Hydr. Engrg.,* ASCE, 123(3), 237-243.

Liu, H. K., Chang, F.M., and Skinner, M. M. (1961). " Effect of bridege construction on scour and backwater." *CER 60 HKL 22*, Colorado State Univ., Civ. Engrg. Section, Ft. Collins, Colo.

Melville, B. W. (1992). " Local scour at bridge abutments." *J. Hydr. Engrg.*, ASCE, 118(4), 615-631.

Melville, B. W. and Coleman, S. E. (2000). *Bridge Scour*. Water Resources Publications, LLC., USA.

Rajaratnam, N., and Nwachukwu, B. A. (1983a). " Flow near groin-like structures." *J. Hydr. Engrg.*, ASCE, 109(3), 463-480.

Rajaratnam, N., and Nwachukwu, B. A. (1983b). " Erosion near groyne structures." *J. Hydr. Res.,* 21(4), 227-287.

Tey, C. B. (1984). " Local scour at bridge abuments." *Rep. No. 329.* School of Engrg. Univ. of Auckland, Auckland, New Zealand.

Van Rijn, L. C. (1984). " Sediment transport, part 1: bedload transport." *J. Hydr. Engrg.,* ASCE, 110(10), 1431-1456.

Wong, W.H. (1982). " Scour at bridge abutments." *Rep. No. 275*. School of Engrg. Univ. of Auckland, Auckland, New Zealand.

Table 1. Maximum equilibrium scour-depth data for vertical-wall abutment (NTU data)

| Author	Run	Q, l/s	γ_s, kN/m^3	D_{50}, mm	u_1, cm/s	L, mm	y, mm	d_{se}/y
Present Study	L1	111.9	1.05	3.10	6.66	70	280.1	0.075
	L2	89.5	1.05	3.10	6.31	70	236.3	0.093
	L3	111.9	1.05	3.10	6.66	140	280.1	0.096
	L4	89.5	1.05	3.10	6.31	140	236.3	0.131
	L5	111.9	1.05	3.10	6.66	240	280.1	0.164
	L6	89.5	1.05	3.10	6.31	240	236.3	0.169
	L7	87.9	1.05	3.10	5.91	240	248.0	0.290
	L8	87.9	1.05	3.10	7.87	240	186.0	0.608
	L9	153.4	1.05	3.10	8.85	320	289.0	0.408
	L10	111.9	1.05	3.10	6.66	440	280.1	0.203
	L11	89.5	1.05	3.10	6.31	440	236.3	0.339
	L12	153.4	1.05	3.10	10.70	440	239.0	0.565
	L13	87.9	1.05	3.10	5.91	440	248.0	0.419
	L14	87.9	1.05	3.10	7.87	440	186.0	1.022
	L15	87.9	1.05	3.10	4.27	880	343.0	0.286
	L16	87.9	1.05	3.10	5.09	880	288.0	0.441
	L17	87.9	1.05	3.10	5.49	880	267.0	0.543
	L18	87.9	1.05	3.10	5.95	880	246.0	0.707
	L19	87.9	1.05	3.10	6.18	880	237.0	0.802
Lim (1997)	S1	216.0	2.65	0.94	24.00	50	150.0	0.240
	S2	219.6	2.65	0.94	24.40	75	150.0	0.507
	S3	127.2	2.65	0.94	21.20	100	100.0	0.570
	S4	218.7	2.65	0.94	24.30	100	150.0	0.673
	S5	188.3	2.65	0.94	25.10	125	125.0	0.928
	S6	230.4	2.65	0.94	25.60	125	150.0	0.753
	S7	162.9	2.65	0.94	18.10	150	150.0	0.367
	S8	214.2	2.65	0.94	23.80	150	150.0	0.733
	S9	216.9	2.65	0.94	24.10	150	150.0	1.067
	S10	280.8	2.65	0.94	31.20	150	150.0	1.533
	S11	292.5	2.65	0.94	32.50	150	150.0	1.667
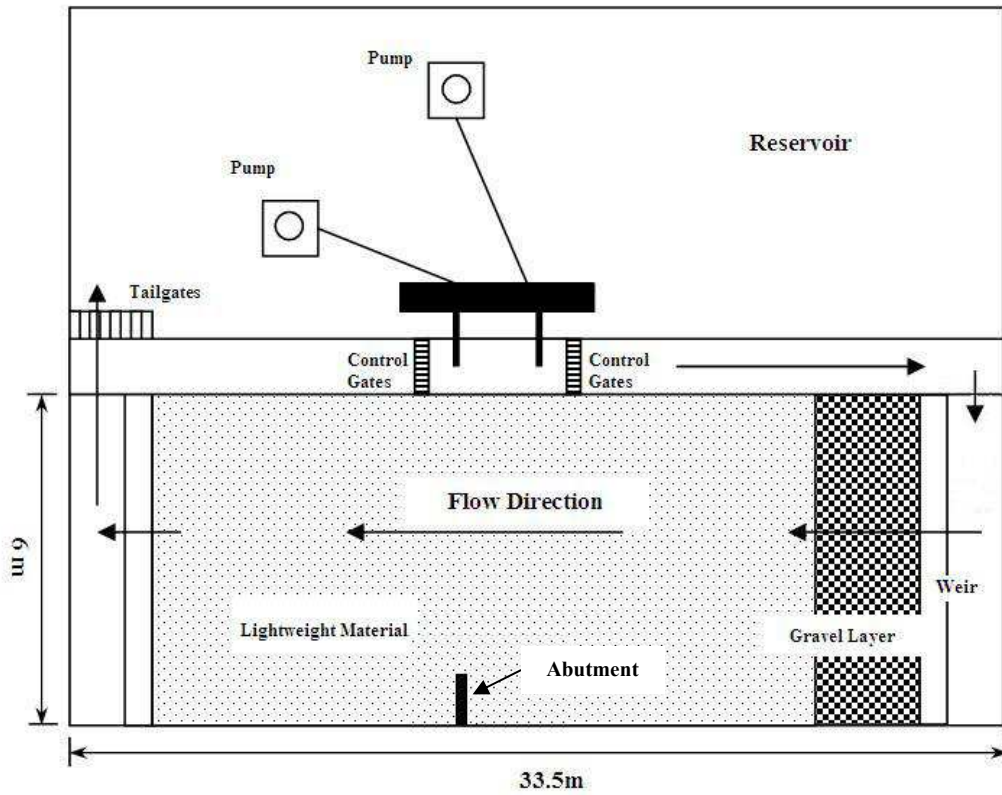
Figure 1. Schematic diagram of experiment layout
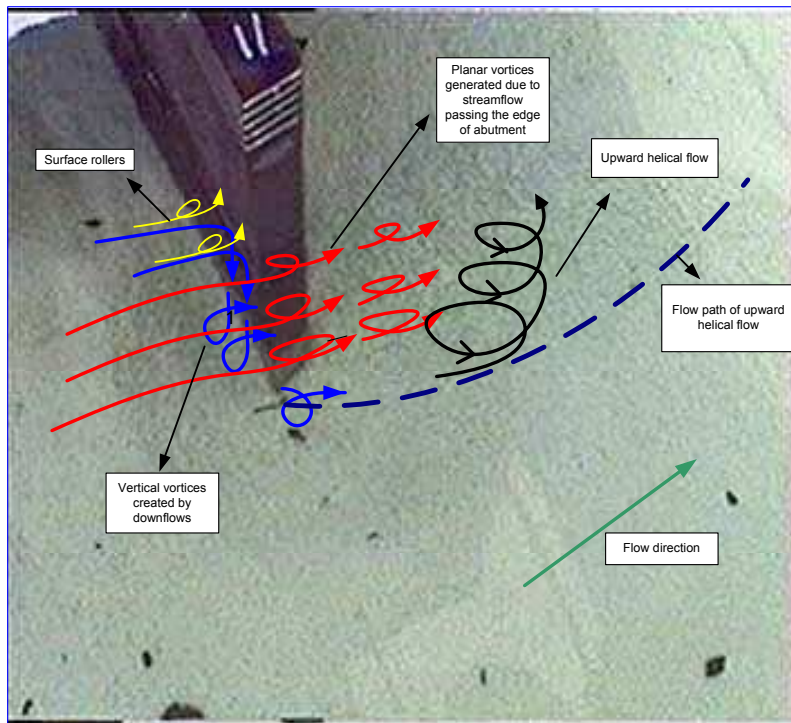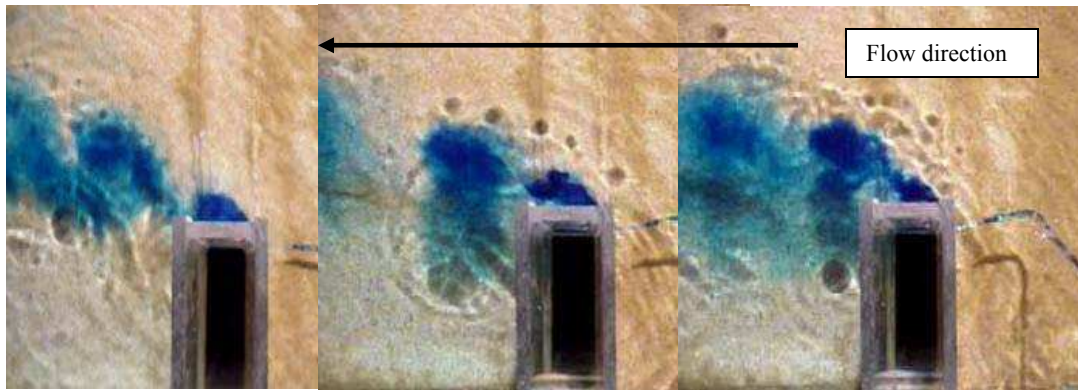

Figure 2. 3-D flow structures and flow paths in abutment scour

Flow direction

(a) Near water surface   (b) Mid-depth   (c) Near Bed

Figure 3. Strength of planar vortices along the edge of abutment (a) near water surface; (b) mid-depth; (c) near bed
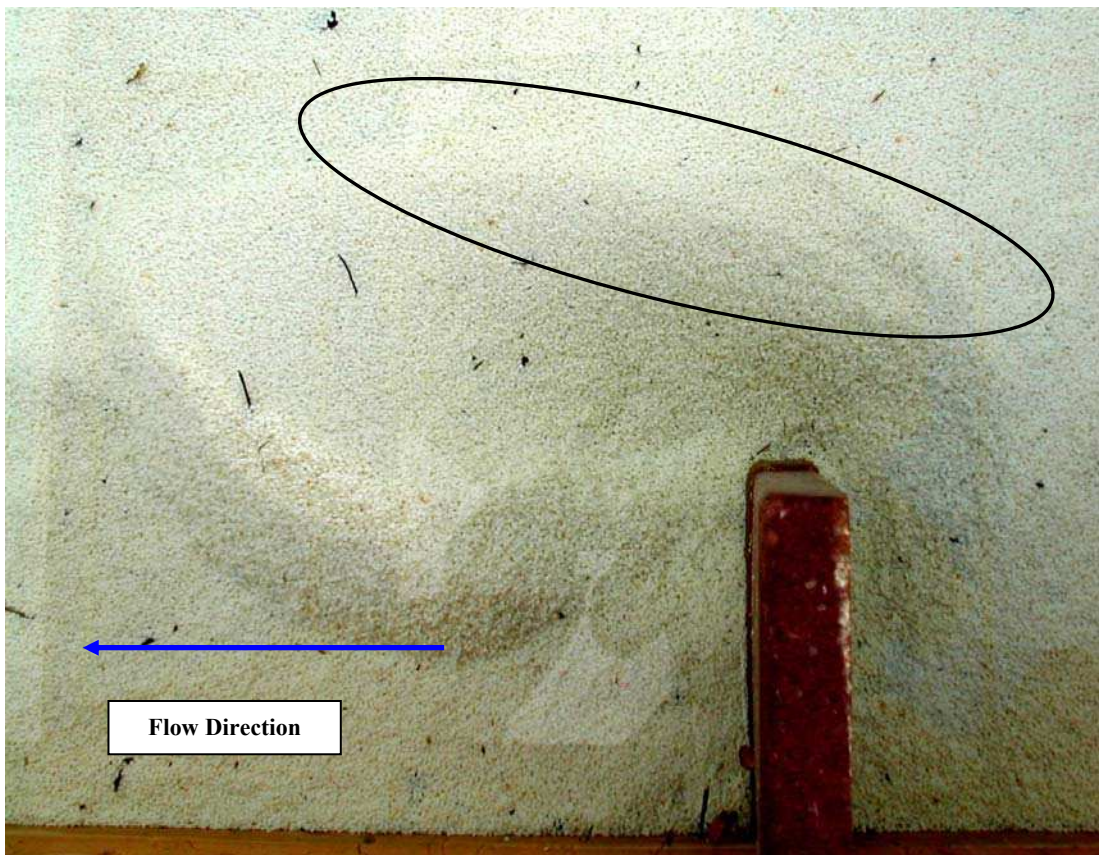

Flow Direction
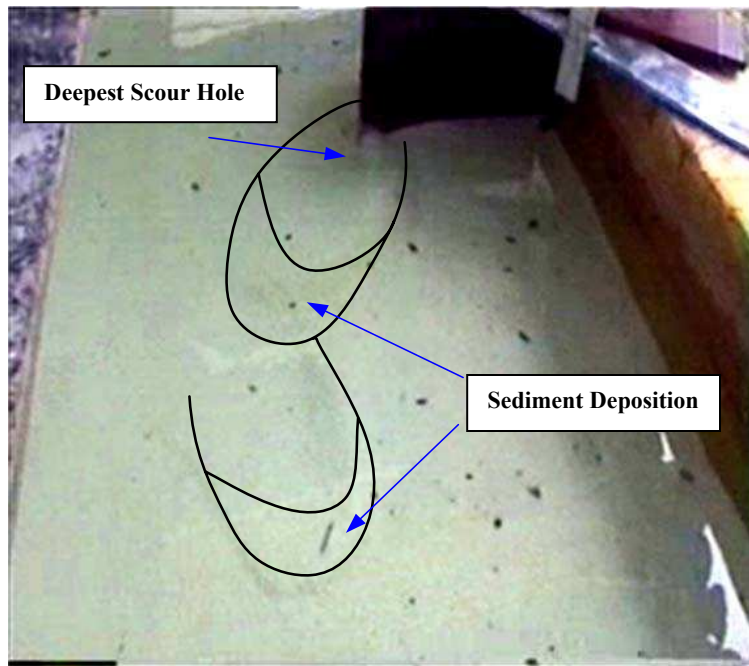
Figure 4. Circled area shows the mild ridge formed by secondary vortices

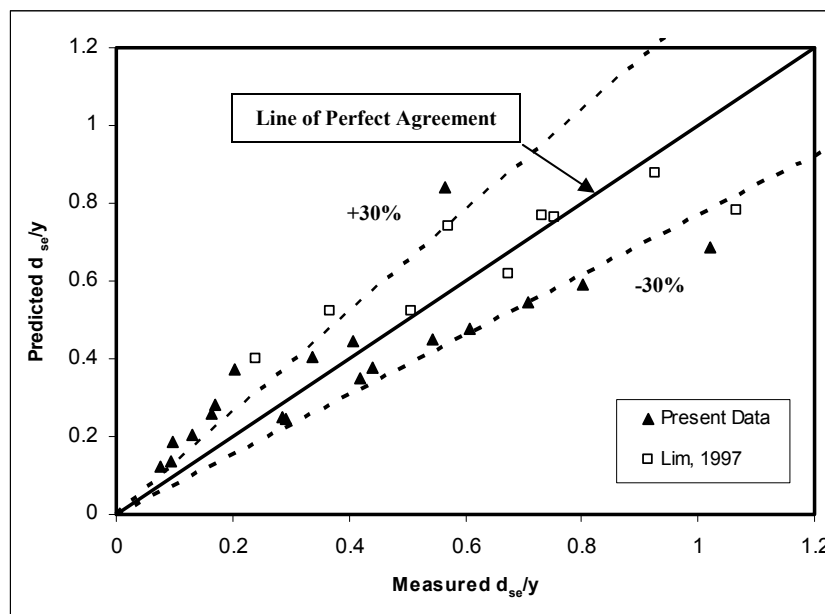**Figure 5. Formation of two scour holes and sediment deposition downstream of the abutment.**

Figure 6. Comparison of maximum scour depth computed using Eqn. (2) with the NTU's measured data summarized in table 1 (NTU data)
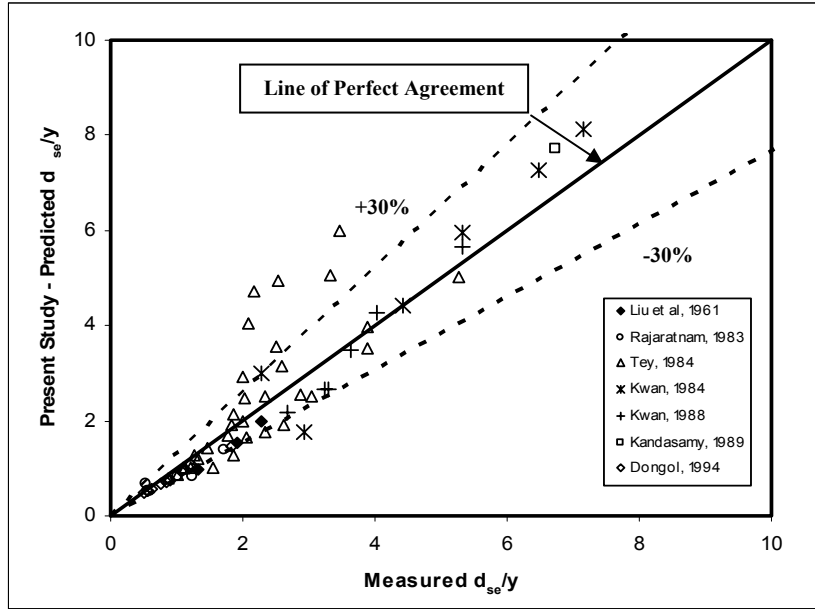
11

Figure 7. Comparison of maximum scour depth computed using Eqn. (3) with measured data by various researchers
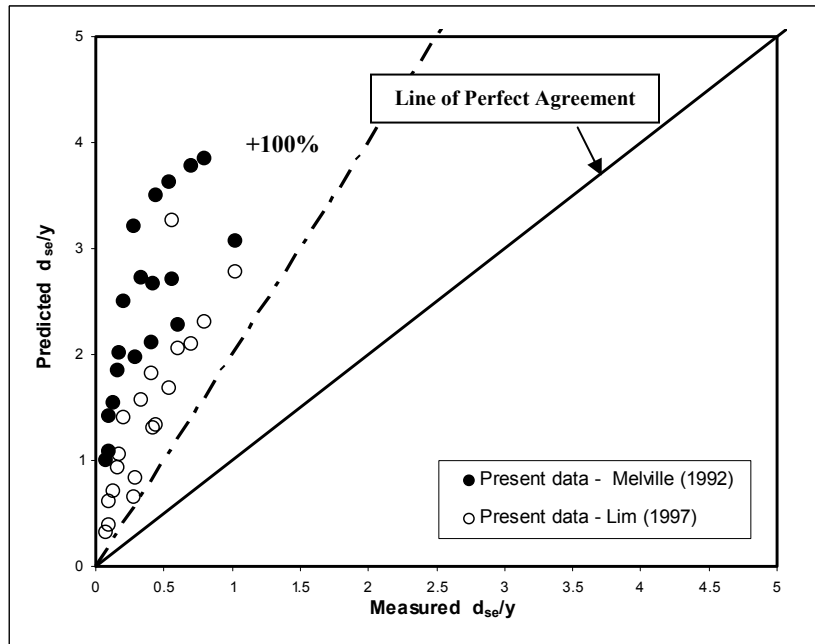

Figure 8. Comparison of maximum scour depth computed using Melville's (1992) Eqn. (4) and Lim's (1997) Eqn. (5) with present measured data